

Supporting Information for "Seasonal predictability of summer melt ponds from winter sea ice surface temperature"

Linda Thielke¹, Niels Fuchs^{2,4}, Gunnar Spreen¹, Bruno Tremblay³, Gerit

Birnbaum⁴, Marcus Huntemann¹, Nils Hutter^{5,4}, Polona Itkin⁶, Arttu

Jutila⁴, Melinda A. Webster⁷

¹Institute of Environmental Physics, University of Bremen, Bremen, Germany

²Center for Earth System Sustainability, Institute of Oceanography, University of Hamburg, Hamburg, Germany

³Department of Atmospheric and Oceanic Sciences, McGill University, Montréal, Québec, Canada

⁴Alfred Wegener Institute, Helmholtz Centre for Polar and Marine Research, Bremerhaven, Germany

⁵Cooperative Institute for Climate, Ocean and Ecosystem Studies, University of Washington, Seattle, WA, USA

⁶UiT The Arctic University of Norway, Tromsø, Norway

⁷University of Alaska Fairbanks, Fairbanks, AK, USA

Corresponding author: L. Thielke, Institute of Environmental Physics, University of Bremen, Otto-Hahn-Allee 1, 28334 Bremen, Germany. (lthielke@iup.physik.uni-bremen.de)

September 28, 2022, 8:39am

Contents of this file

1. Introduction
2. Warm temperature anomalies: Figure S1, Table S1 to S2
3. Details on the thermodynamic model: Equation S1 to S4, Table S3
4. Snow and ice conditions: Figure S2 to S3

References

- Untersteiner, N. (1964). Calculations of temperature regime and heat budget of sea ice in the central Arctic. *Journal of Geophysical Research*, *69*(22), 4755–4766. doi: <https://doi.org/10.1029/JZ069i022p04755>
- Yu, Y., & Rothrock, D. (1996). Thin ice thickness from satellite thermal imagery. *Journal of Geophysical Research: Oceans*, *101*(C11), 25753–25766. doi: <https://doi.org/10.1029/96JC02242>

Introduction

Here we show additional Figures and Tables which support the findings presented in the main article. The display material is grouped by topic for an easier reference in the article.

Warm temperature anomalies

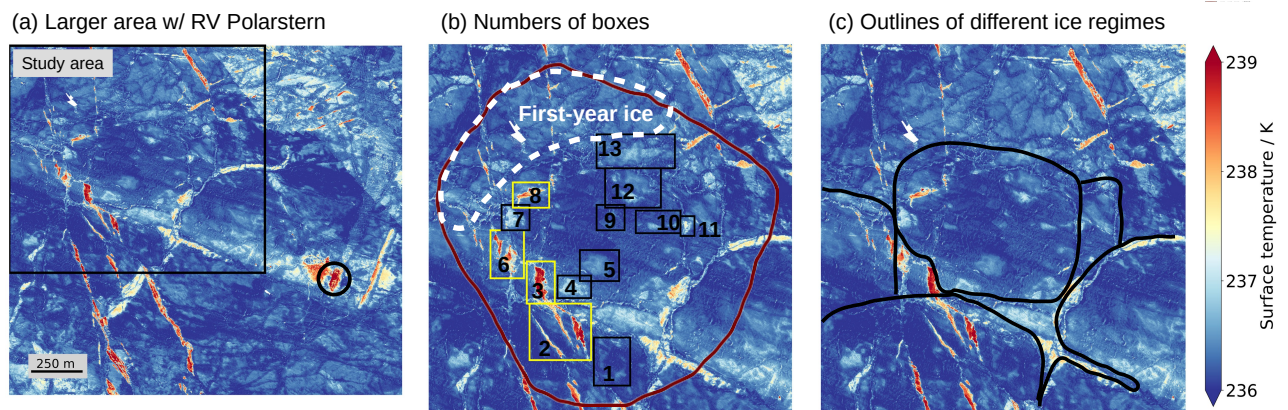


Figure S1. Surface temperature maps on 21 January 2020 with (a) a larger area selection with the study area (black box) in context to RV *Polarstern* (black circle), (b) the same as Figure 1 (a), but with the numbers of the boxes to have the possibility to refer to the single boxes. The white dashed line shows the area which is first-year ice while the rest of the floe area is second-year ice. (c) shows the outline of different ice regimes in the study area.

Table S1. Box properties: warm anomaly type, temperature difference $\Delta T_{s,obs}$, box size, shape description, and additional comments. The types are i) refrozen leads (RL) or ii) topographically controlled (TC).

Box No.	Type	$\Delta T_{s,obs}$ / K	Box size (x*y) / m	Shape	Comment
1	TC	0.3	130*170	oval	several parts
2	RL	2.0	220*200	elongated	three parts
3	RL	2.5	100*150	elongated	-
4	TC	0.4	120*80	oval	Warmer outer circle
5	TC	0.3	140*110	oval	scattered
6	RL	2.0	120*170	elongated	-
7	TC	0.7	180*90	oval	-
8	RL	1.7	130*90	elongated	-
9	TC	0.5	100*90	oval	scattered
10	TC	0.4	160*80	oval	scattered
11	TC	0.7	50*70	oval	-
12	TC	0.6	200*140	oval	two parts
13	TC	0.3	280*120	oval	-

Table S2. Temperature difference (Warm anomaly - Surroundings) at the ten helicopter survey dates between 30 November 2019 and 12 February 2020 for the warm anomalies in the RL-case (refrozen lead, Box 3) and TC-case (topography controlled, Box 5). The refrozen lead only appears after 28 December 2020 because of ice dynamics.

Date	RL-case $\Delta T_{s,obs}/K$	TC-case $\Delta T_{s,obs}/K$
30 Nov 19	-	0.2
24 Dec 19	-	0.8
25 Dec 19	-	1.0
28 Dec 19	-	0.6
07 Jan 20	11.8	1.3
16 Jan 20	2.0	0.5
21 Jan 20	2.5	0.3
28 Jan 20	2.3	1.0
04 Feb 20	2.4	0.6
12 Feb 20	0.5	0.2

Details on the thermodynamic model

The definition of upwelling longwave radiation $F_{\text{LW,up}}$ is:

$$F_{\text{LW,up}} = \sigma T_s^4 \quad (\text{S1})$$

with the Stefan-Boltzmann constant σ and the surface temperature T_s .

This is linearized by Taylor series expansion to:

$$\sigma T_s^4 = \sigma[f(T_0) + (T_s - T_0)f'(T_0)/1!] = \sigma[T_0^4 + (T_s - T_0)4T_0^3] = a + bT_s \quad (\text{S2})$$

with $a = -3\sigma T_0^4$, and $b = 4\sigma T_0^3$ as coefficients of linearization based on the background temperature T_0 which is at 240 K as best guess. The results are tested to be not sensitive to the variation of T_0 in a reasonable temperature range (below the freezing point).

The definition of conductive heat flux F_{cond} is:

$$F_{\text{cond}} = \frac{(T_s - T_w)}{\frac{h_i}{k_i} + \frac{h_s}{k_s}}. \quad (\text{S3})$$

The definition of sensible heat flux F_{sens} is

$$F_{\text{sens}} = c(T_s - T_a) = \rho_{\text{air}}c_p C_s(T_s - T_a) \quad (\text{S4})$$

with the sensible transfer coefficient c , the air density ρ_{air} , the heat capacity c_p , the turbulent transfer coefficient C_s , and the 2 m air temperature T_a .

Table S3. Input parameter for model. These are the values for 21 January 2020.

Variable	Long name	Value	Comment
T_a^*	2 m air temperature	243.5 K	on floe at recording time
u^*	10 m wind speed	5.4 m s^{-1}	on floe at recording time
$F_{\text{LW,down}}^*$	Downwelling longwave radiation	193.6 W m^{-2}	on floe at recording time
$h_{\text{i,level}}$	Level ice thickness	$1.11 \pm 0.09 \text{ m}$	from transect
$h_{\text{s,level}}$	Level snow depth	$0.16 \pm 0.06 \text{ m}$	from transect
$h_{\text{i,deformed}}$	Deformed ice thickness	$3.74 \pm 1.91 \text{ m}$	from transect
$h_{\text{s,deformed}}$	Deformed snow depth	$0.29 \pm 0.13 \text{ m}$	from transect
k_i	Thermal conductivity of ice	$2.0 \text{ W m}^{-1} \text{ K}^{-1}$	after Untersteiner (1964)
k_s	Thermal conductivity of snow	$0.3 \text{ W m}^{-1} \text{ K}^{-1}$	common literature value
ρ_a	Air density	1.44 kg m^{-3}	for $p=1013 \text{ hPa}$, $T=245 \text{ K}$
T_w	Sea water temp. at freezing point	271.35 K	-
T_0	Background temp. for linearization	240 K	best guess
σ	Stefan-Boltzmann constant	$5.67 \times 10^{-8} \text{ W m}^{-2} \text{ K}^{-4}$	-
c_p	Specific heat capacity of air	$1000 \text{ W s K}^{-1} \text{ kg}^{-1}$	-
C_s	Sensible turbulent transfer coefficient	0.00175	Yu and Rothrock (1996)

Snow and ice conditions

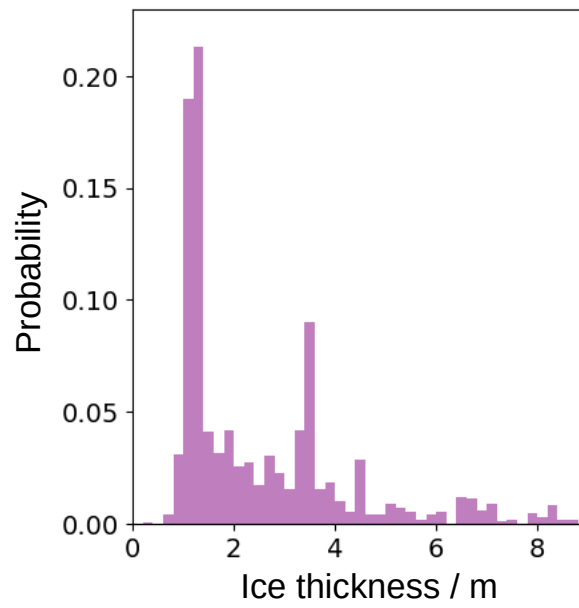


Figure S2. Histogram of the ice thickness retrieved from an ice thickness transect over the study area on 07 January 2020.

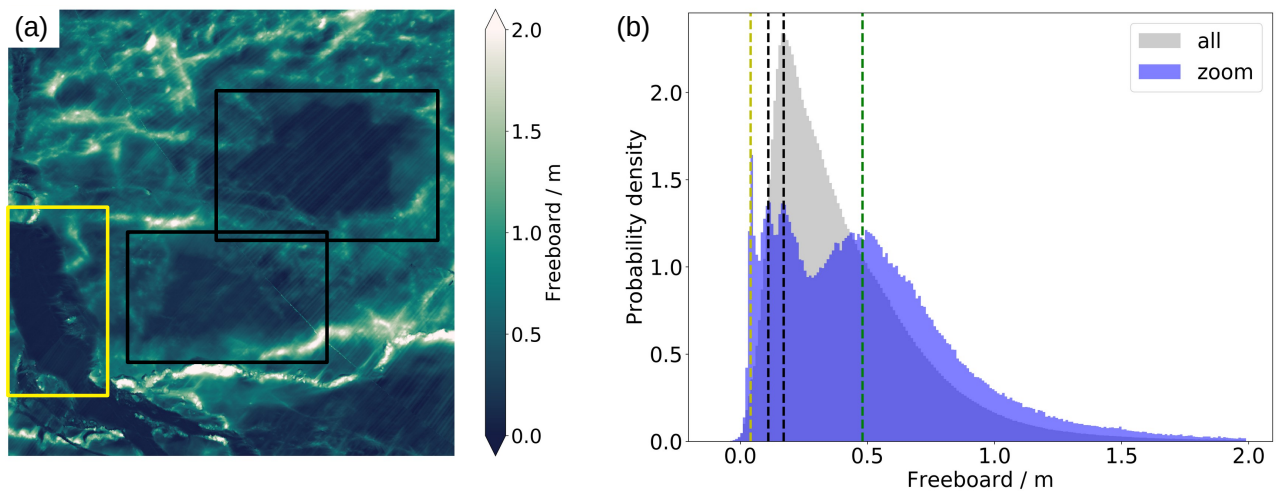


Figure S3. Freeboard map from ALS for a selection of the study area with a size of $300\text{ m} \times 300\text{ m}$. (a) Map for the area of the melt pond boxes 3, 4, and 5, and (b) histogram of the freeboard of the full study area (gray) and the area of (a) in blue with modes (vertical lines) of the warm anomalies (yellow/black dashed) as well as the surroundings (green dashed).